

Effect of surface modifications of carbon black (CB) on the properties of CB/polyurethane foams

Mao Peng · Mingxing Zhou · Zhijiang Jin ·
Weiwei Kong · Zhongbin Xu · Damien Vadillo

Received: 15 July 2009 / Accepted: 14 November 2009 / Published online: 1 December 2009
© Springer Science+Business Media, LLC 2009

Abstract The effect of surface modifications of carbon black (CB) on its dispersion in polyether polyol and CB/polyurethane (PU) foams and the properties of the CB/PU composite foams was investigated. Pristine CB (p-CB) was oxidized in nitric acid to obtain oxidized CB (o-CB), and then by the esterification reaction between the carboxyl groups of o-CB and the hydroxyl groups of polyether polyol, polyol grafted CB (g-CB) was obtained. Optical microscopy, scanning and transmission electron microscopy observations showed that surface modifications effectively improved the dispersion of CB in polyether polyol and in the final composite foams. Compared with the p-CB/PU foams, the o-CB/PU and g-CB/PU composite foams exhibited improved conductivities, storage moduli, and increased glass transition temperatures. The compressive strengths of the p-CB/PU and o-CB/PU composite foams decreased with the increase of filler contents, but g-CB has no negative effect on the compressive strength even at a filler content as high as 8 phr. Furthermore, the cell sizes for the o-CB/PU and g-CB/PU composite foams were more uniform than those of p-CB/PU foams.

Introduction

Polyurethane foams (PUFs) exhibit versatile properties such as outstanding mechanical strength, heat resistance, and low density. The properties of PUFs can be tailored by adjusting the combinations of the monomeric materials to meet diversified demands for various applications. Meanwhile, the fabrication processes of PUFs are relatively simple and flexible, which enable PUFs to be used in a remarkably broad range of applications [1], such as heat insulation materials [2], structure materials [3], furniture, car seating, packaging materials and biomaterials [4].

Previous studies have shown that incorporation of a variety of fillers is effective to improve the properties and extends the applications of polymeric foams. For example, the tensile strength of polymeric foams can be enhanced by adding glass fibers [5] or carbon fibers [6]. The fracture toughness can be enhanced by adding hollow microspheres [6]. Carbon nanotubes [7, 8] and clays [9–11] were also used to improve the electric conductivity and mechanical properties, respectively. However, uniform dispersion of filler particles (especially nanoparticles) in polymer matrices is a challenge for the preparation of nanocomposites. Therefore, many efforts have been devoted to solve this problem [12–17]. Yang et al. [7] used a surfactant to disperse carbon nanofibers into a toluene solution of polystyrene under ultrasonication. The resultant composite foams had typical percolation behavior and became static dissipative when the filler contents were above 2 wt%. Li et al. [8] mixed purified carbon nanotubes (CNTs) with polyether polyol at 100 °C by mechanical stirring and ultrasonication, and the prepared CNT/PU foams exhibited a quite low density of 0.05 g cm⁻³ and a desirable conductivity of approximately 4.3 × 10⁻⁵ S m⁻¹. Cao et al. [9] synthesized montmorillonite/PU foams in which the

M. Peng · M. Zhou · Z. Jin · W. Kong · Z. Xu (✉)
Faculty of Engineering, Zhejiang University, Hangzhou
310027, People's Republic of China
e-mail: xuzhongbin@zju.edu.cn

M. Peng
e-mail: pengmao@zju.edu.cn

Z. Xu · D. Vadillo
Department of Chemical Engineering and Biotechnology,
University of Cambridge, Cambridge CB2 3RA, UK

D. Vadillo
e-mail: dv244@cam.ac.uk

functional groups of the organic modifiers, synthesis procedure, and molecular weight of polyols were found to strongly affect the morphology and properties of the foams. The presence of clay resulted in an increased cell density and reduced cell sizes in comparison with pure PU foams. In recent years, we have also studied the influence of surface modifications of clay on the properties of PU foams [10, 11].

Carbon black (CB) has a long history of being used as fillers of plastics [18, 19] and rubbers [20]. CB/PU foams are also widely used for structural and conductive applications [21]. However, because of the strong interparticle interactions, CB particles tend to form agglomerates in polymer matrices, which usually reduces the properties of the composites. Therefore there has been great interest in the improvement of the dispersion of CB in PU foams. It has been demonstrated that ball milling has a better effect on CB dispersion than the mechanical stirring and ultrasonication [16]. Coupling agents have been used to improve the mechanical and conductive properties of CB/PU foams [22]. It has also been reported that the dispersion of CB can be improved by oxidation [23] or grafting [24].

In this study, we prepared carboxylated CB (o-CB) by oxidizing CB in nitric acid and polyether polyol grafted CB (g-CB) by the esterification reaction between o-CB and polyether polyol. The effect of chemical modifications on the dispersion of CB in polyols and PU composites was investigated. The bearing of chemical modifications and aggregate sizes on conductivities, mechanical properties, and cell size distributions of the CB/PU foams was also discussed.

Experimental

Materials

Polyether polyol (ZS-4110, Jiangsu GPRO Group Co., Ltd., China) was made from poly(propylene oxide), sucrose, and glycerin, with a typical hydroxyl value of $434 \pm 30 \text{ mg g}^{-1}$ of KOH; a viscosity (at 25 °C) of 5.092 Pa s; a density (at 25 °C) of 1.10 g mL^{-1} , and a water content below 0.15 wt%. Polyisocyanate (commercial brand MR100), with a –NCO content of 30 wt% and a density (at 25 °C) of 1.20 g mL^{-1} was supplied by Nippon Polyurethane Industry Co., Ltd., Japan. The catalyst of A-33 (33 wt% triethylene diamine in dipropylene-glycol) and dibutyltin dilaurate were purchased from Youth Advanced Material Co., Ltd., Shanghai, China. The surfactant (AK8818, Dymatic Shichuang Chemical Co., Ltd., Nanjing, China) was a kind of polysiloxane-polyether copolymer. 4-dimethylamino pyridine (DMAP, Dow Chemical, USA)

was used as the catalyst of the esterification reaction. The blowing agent of the PUFs was distilled water. Three types of CBs were used to prepare CB/PU foams. One was pristine CB, (N550, Degussa Chemical Co., Qingdao, China, denoted as p-CB in this article), furnace black with an average diameter of 80 nm and pour density of 0.365 g mL^{-1} . The others were o-CB and g-CB.

Sample preparations

In order to prepare o-CB, p-CB (10 g) was dispersed in concentrated nitric acid (210 mL), and the mixture was heated to 100 °C and remained for 12 h under magnetic stirring. o-CB was collected after being sufficiently washed with distilled water and dried in a vacuum oven at 80 °C for 24 h.

g-CB was prepared by the esterification reaction between the carboxyl groups on the surface of o-CB and the hydroxyl groups in the polyether polyol molecules. 22.3 g of o-CB, 120 g of polyester polyol, and 200 mL of toluene were added into a 500 mL three-necked flask and stirred for 1 h at 100 °C under the protection of N₂. Then, 0.231 g of DMAP was added, and the esterification reaction was allowed to perform for 12 h. After reaction, the system was heated to 120 °C to remove toluene. The obtained g-CB was filtered and washed 10 times with ethanol to remove any unreacted polyether polyol and then dried in a vacuum oven.

The CBs (p-CB, o-CB, and g-CB) were mechanically ground into fine powder before use. The pure PU foams and CB/PU foams were prepared by a one-shot process. Precalculated amount of CB was first mixed with polyether polyol (100 phr). Then, the polyether polyol/CB mixture, polyisocyanate, and the mold with inside dimensions of $200 \times 150 \times 30 \text{ mm}$ were heated in an oven at 40 °C for 1 h. Subsequently, A-33 (0.8 phr), water (1 phr), surfactant (3 phr), and dibutyltin dilaurate (0.05 phr) were added into the polyether polyol/CB mixture and stirred intensively for 5 min. After that, polyisocyanate (135 phr) was added. The mixture was stirred for another 20 s and then quickly poured into the mold. The NCO/OH ratio was 1.05:1. The added polyisocyanate reacted with water to produce CO₂ which initiated the foaming process. After foaming at 40 °C for 20 min, the foams were transferred into an oven at 80 °C for 12 h to complete the curing reaction. p-CB/PU, o-CB/PU, and g-CB/PU foams were prepared for comparison.

In order to calculate the volume fraction of CB, the density of p-CB, o-CB, and g-CB was experimentally determined by the standard liquid displacement pycnometer method (ISO 8130-3). The result was presented in Table 1.

Table 1 Volume fraction of p-CB, o-CB, and g-CB

CB content	Volume content (%)		
	p-CB/PU	o-CB/PU	g-CB/PU
2 phr	0.65	0.63	0.68
4 phr	1.28	1.25	1.35
6 phr	1.91	1.87	2.01
8 phr	2.54	2.47	2.66

Characterization

The quantity of carboxyl groups on the surfaces of p-CB and o-CB was evaluated by Boehm titration [25], in which 1.0 g of CB was added to 50 mL of 0.05 mol L⁻¹ aqueous solution of NaHCO₃. The mixture was stirred for 48 h at room temperature. The liquid was filtered, and then, the residual concentration of NaHCO₃ in the liquid was measured by titration with 0.05 N HCl. The quantity of carboxyl groups on o-CB was calculated according to the amount of NaHCO₃ consumed by o-CB and assuming that NaHCO₃ only reacts with the carboxyl groups on the surface of o-CB particles.

The carbon and hydrogen element analysis of CB was examined on a Flash EA1112 Elemental Analyzer (CE Instruments, UK). Each sample was analyzed twice, and the average value was employed for analysis.

Thermogravimetric analysis (TG) of CB was conducted on a TA SDT Q600 thermal analyzer (TA Instruments, New Castle, DE, USA) under a nitrogen atmosphere. All the samples were heated to 120 °C and left at that temperature for 10 min, and then heated to 600 °C at a heating rate of 10 °C min⁻¹.

The dispersion of p-CB, o-CB, and g-CB in polyether polyol was observed by XP-J203E optical microscopy (Changfang Optical Instrument Co., Ltd., Shanghai, China). After CB and polyether polyol were mixed and stirred for 5 min, a drop of the mixture was dripped onto a glass slide and compressed by a cover slip. The morphology of CB agglomerates in the polyol was recorded before and after the samples were kept for 12 h.

The cellular morphology of the foams was investigated by scanning electron microscopy (SEM, JSM-5510LV, JEOL, Japan). Foam samples were cut along the rising direction of the foams at ambient temperature, and the fracture surfaces were sputter-coated with gold for the SEM observation. Image analysis was performed on the SEM images using Image-Pro Plus software (Media Cybernetics, USA.) to obtain the average cell sizes and the distributions of the cell sizes [26]. The “cell size” was determined as “average length of diameters measured at 2 degree intervals and passing through cell’s centroid” and

the “average cell size” was the number-average cell diameter of about 300 cells per sample. The dispersion of CB particles in the cell walls of PUFs was observed by a field-emission SEM (FESEM, SIRION-100, FEI, the Netherlands), and the compositions of the modified CBs were measured by an energy dispersive X-ray (EDX) spectrometer attached to the FESEM.

The dispersion of CB in the composite foams was further examined by transmission electron microscopy (TEM, JEM-1200EX, JEOL, Japan). The specimens were embedded in epoxy resin and cut into thin film with a thickness of 70–90 nm by using a Diatome diamond knife at room temperature. Image analysis was also performed on the TEM images using Image-Pro Plus 5.0 software to obtain the average size and size distribution of CB aggregates. Around 50 aggregates per sample were counted for analysis.

The volume resistivity of the composite foams was determined by a ZC 36-type high resistance meter (Shanghai Precision & Scientific Instrument Co. Ltd., China) at room temperature. The thickness of the specimens was 4 mm. The data reported here were the means of experiments performed in quintuplicate.

The dynamic mechanical properties of the foams were measured on a dynamic mechanical analyzer (DMA 242C, Netzsch, Germany) in a dual cantilever mode at a frequency of 1 Hz. The temperature was heated from 30 to 220 °C at a heating rate of 3 °C min⁻¹. The sample dimension was 30 mm × 12 mm × 3 mm.

The compressive strengths were measured by an RGT-X010 universal testing machine (Shenzhen Reger Instrument, China) at a constant rate of 2 mm min⁻¹ at ambient temperature. The specimen had a dimension of 35 mm × 35 mm × 30 mm. Five specimens were tested for each composition.

Results and discussion

Modification of CB

In order to determine the effect of chemical oxidation on CB, the Boehm titration was conducted. The result showed that the concentrations of carboxyl groups on the surface of p-CB and o-CB were 0.496 mmol g⁻¹ and 1.05 mmol g⁻¹, respectively, indicating that chemical oxidation by nitric acid resulted in an increase in the content of carboxyl groups on the surface of CB. The introduced carboxyl groups provided the possibility of grafting polyol onto o-CB.

As shown in Table 2, the result of element analysis indicated that the weight percent of C element decreased, while that of H increased after oxidation. The element

Table 2 Element analysis results of p-CB, o-CB, and g-CB

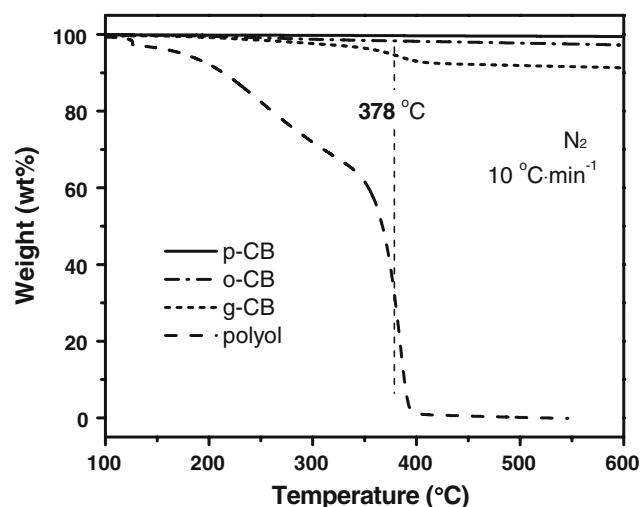
Items	C (wt%)	H (wt%)	N (wt%)	Other (wt%)
p-CB	97.05	0.26	0	2.69
o-CB	95.06	0.38	0	4.56
g-CB	92.07	0.95	0	6.98

Table 3 EDX data for p-CB, o-CB, and g-CB

Element	C		O	
	wt%	at%	wt%	at%
p-CB	96.68	97.62	2.96	2.24
o-CB	95.75	97.02	3.58	2.72
g-CB	90.07	92.45	9.65	7.44

contributing to the raise of the weight percent of “other elements” should be O, indicating that CB was successfully oxidized by nitric acid and the content of oxygen increased after oxidation and esterification. The results of EDX (Table 3) were in good consistency with that of element analysis, which showed that the content of oxygen increased after the oxidation and esterification reactions, indicating that polyester polyol was successfully grafted onto CB.

Furthermore, the TG curves of CB and polyether polyol were also used to determine whether the polyester polyol was grafted onto CB after esterification. As shown in Fig. 1, p-CB remained stable without significant weight loss up to 600 °C, while o-CB exhibited a slight weight loss and g-CB exhibited larger weight loss than o-CB. The temperature range where the maximum weight loss rate of

**Fig. 1** TG curves of p-CB, o-CB, g-CB, and polyol

polyether polyol occurred was between 362 and 389 °C. Correspondingly, the temperature range of g-CB was between 375 and 403 °C, which is similar to that of polyether polyol, indicating that polyol was grafted on the surface of CB [27]. The residual weights at 600 °C for p-CB, o-CB, g-CB, and polyol were 98.9, 95.7, 89.5, and 0 wt%, respectively. Accordingly, the amount of carboxyl groups can be calculated to be about 3.2 wt%, which is in satisfactory agreement with the results obtained by titration, element analysis, and EDX. The amount of polyol grafted onto the surface of o-CBs was about 9.4 wt%.

Dispersion of CBs in polyether polyol and the composite foams

Previous studies have demonstrated that the dispersion of carbon nanoparticles in a polar solvent can be improved by chemical modification [24, 28]. Figure 2 shows that the dispersion of both o-CB and g-CB in polyol is more uniform than that of p-CB. After being kept standing for 12 h at room temperature, p-CB formed large aggregates in polyol (Fig. 2b), while o-CB and g-CB remained homogeneously dispersed (Fig. 2d, f). The better dispersion of o-CB in polyol can be attributed to two major reasons. First, the polar groups like –OH and C=O on the surface of CB created during oxidation [29, 30] can interact with the –OH groups and polar –CH₂–O–CH₂– segments in the polyether polyol through hydrogen bonds [31], and subsequently improve the compatibility of CB and polyol. Secondly, according to previous studies, a large number of pores could be generated in CB particles during the oxidation process, leading to enhanced roughness and surface area of CB. Therefore, the CB agglomerates became fluffier and easier to disperse in the polyol media [32]. Furthermore, the improved dispersion of g-CB in polyol is obviously attributed to the good compatibility of polyether polyol and the g-CB.

Since o-CB and g-CB dispersed better in polyol than p-CB, they could also disperse more homogeneously in composite foams, which was confirmed by SEM and TEM images. In Fig. 3a, d some large aggregates in the cell walls of p-CB/PU foams are observed. In Fig. 3b, e the sizes of the o-CB aggregates are much smaller than those of p-CB aggregates, demonstrating that the chemical oxidation of CB improved its dispersion in o-CB/PU foams. For g-CB/PU foams, the g-CB aggregates are hardly observed on the surface of the cell walls (Fig. 3c) and the sizes of aggregates (see Fig. 3f) are also much smaller than that of p-CB aggregates, because of the improved dispersion and the interfacial adhesion between g-CB and the PU matrix. The size and size distribution of CB aggregates are given in Fig. 4. The aggregate size is 350, 256, and 224 nm

Fig. 2 Optical microscope images of polyol/CB (weight ratio: 50/2) mixture: **a** polyol/p-CB (as prepared), **b** polyol/p-CB (kept for 12 h), **c** polyol/o-CB (as prepared), **d** polyol/p-CB (kept for 12 h), **e** polyol/g-CB (as prepared), **f** polyol/g-CB (kept for 12 h)

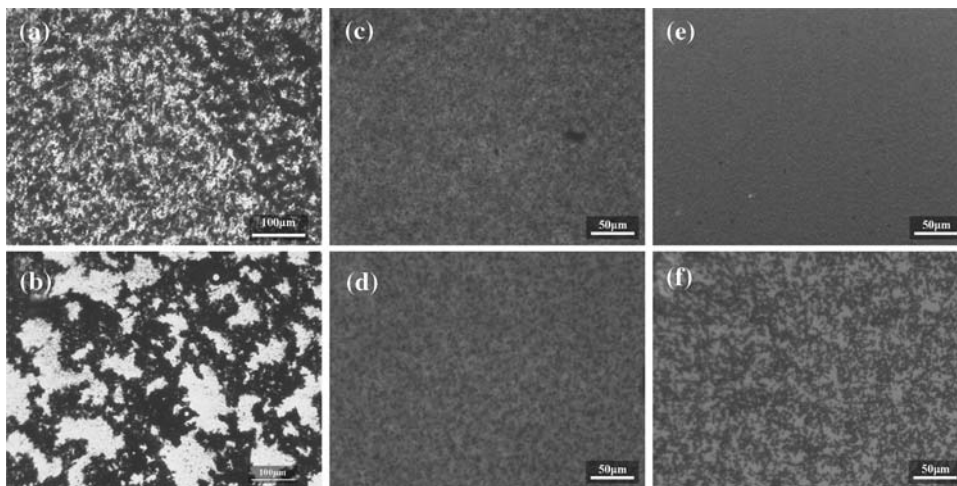
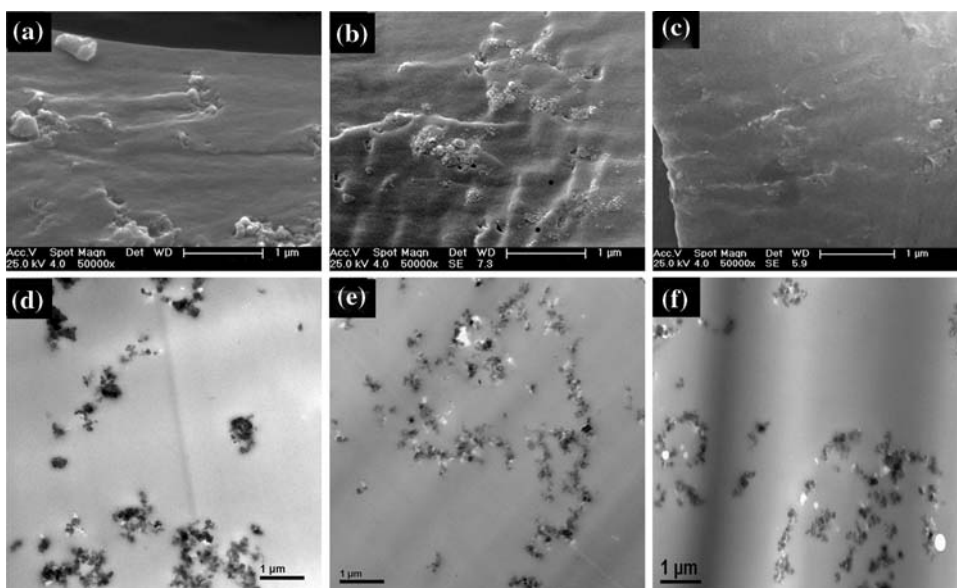


Fig. 3 SEM images of **a** p-CB/PU, **b** o-CB/PU, and **c** g-CB/PU foams and TEM images of **d** p-CB/PU, **e** o-CB/PU, and **f** g-CB/PU foams with a filler content of 6 phr



for p-CB, o-CB, and g-CB, respectively. Moreover, the size distribution becomes narrower after surface modifications.

Properties of CB/PU foams

The electrical properties of the composite foams with different CB contents are presented in Fig. 5. The volume resistivity of the p-CB/PU foams did not decrease significantly with the increase of the p-CB content when the filler contents were below 8 phr. However, for o-CB/PU systems, when the amount of o-CB reached 4 phr the resistivity reduced dramatically. Moreover, when the amount of o-CB was 8 phr, the volume resistivity of o-CB/PU foams decreased to below $10^9 \Omega \text{ m}$, indicating that oxidation was effective to improve the electrical conductivity and the composite foams fabricated by this method could be qualified for static dissipative applications [33]. As previously mentioned, p-CB forms large agglomerates in p-CB/

PU foams (Fig. 3a), so continuous conductive paths are difficult to form at low p-CB contents. Owing to the improved interactions between o-CB and the PU matrix, o-CB aggregates are much smaller in size and can be dispersed more homogeneously in PU matrix [34]. Therefore, the average distance among the conductive CB aggregates is reduced and the formation of continuous conductive paths in the PUF matrix is easier, which results in an improved conductivity at lower filler contents of o-CB. As for the g-CB/PU foams, the volume resistivity is lower than that of p-CB/PU foams, but higher than that of o-CB/PU foams. A possible explanation is that the grafted polyol on the surface of g-CB contributes to the dispersion of g-CB, but reduces the conductivity of g-CB and makes the formation of continuous conductive path in the PU/g-CB foams more difficult.

The dynamic mechanical properties of CB/PU foams were investigated. The storage modulus (E') and loss

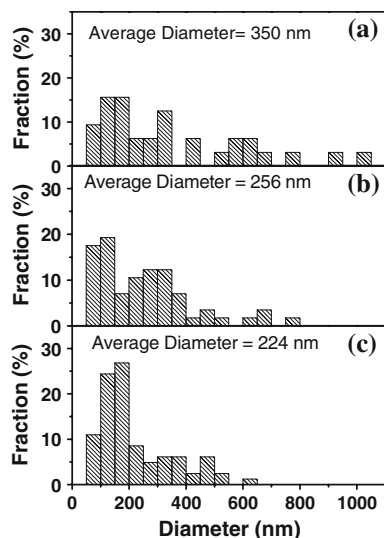


Fig. 4 Aggregate size histograms of **a** p-CB, **b** o-CB, and **c** g-CB at a filler content of 6 phr in the PU matrix

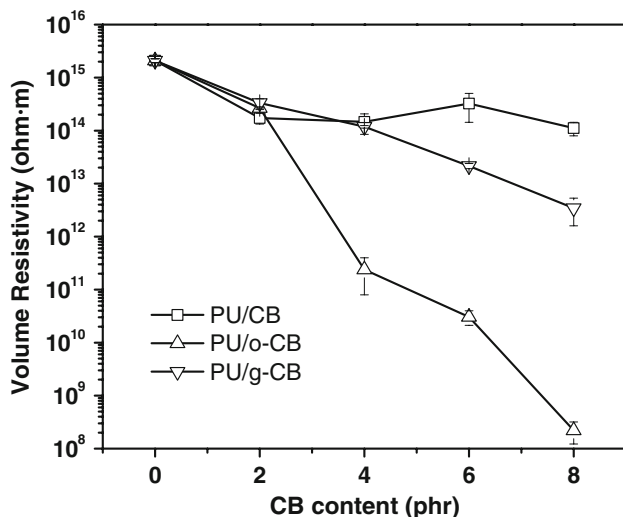


Fig. 5 Electrical properties of p-CB/PU, o-CB/PU, and g-CB/PU foams as a function of CB content

tangent ($\tan\delta$) curves are presented in Fig. 6. The differences in storage modulus values and glass transition temperature (T_g), corresponding to the peaks of the $\tan\delta$ curves, provided useful information on the interaction between CB fillers and the matrix. For all CB/PU foams, the storage modulus increased. However, modified CB, particularly g-CB, was much more effective in increasing the storage moduli than p-CB. The same tendency was found in the T_g values, which are 176.5 °C, 179.1 °C, 181.2 °C, and 183.9 °C for blank PU, PU/p-CB, PU/o-CB, and PU/g-CB foams, respectively. The simultaneous increase in both E' and T_g for o-CB/PU and g-CB/PU foams can be attributed to the improvement of CB dispersion and the interactions between CB particles and the

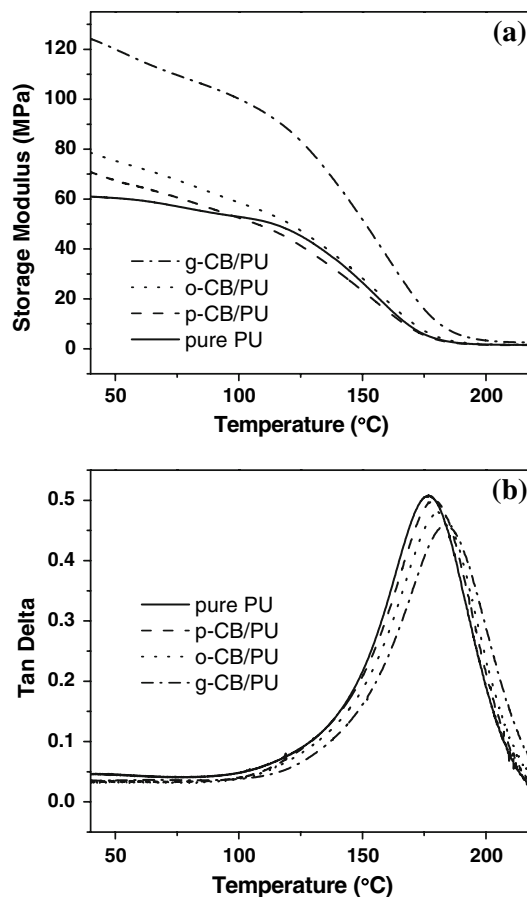


Fig. 6 Temperature dependence of **a** storage modulus (E') and **b** loss tangent ($\tan\delta$) for PUFs, p-CB/PU, o-CB/PU, and g-CB/PU foams with a filler content of 6 phr

PU matrix. Owing to the better dispersion of o-CB and g-CB particles the interface area between CBs and the PU matrix is greatly enlarged, and the molecular movement of PU matrix is less active so that the storage modulus increases and T_g shifts to higher temperature and the area of $\tan\delta$ peak decreases.

Most CB particles exist in the form of aggregates in the composite foams due to their small sizes and enormous surface energy. The aggregates usually tend to decrease the strength of the composite foams [35] owing to the inferior mechanical strength of aggregates and the poor interaction between CB aggregates and the polymer matrix. Figure 7 shows that both the amount of CB and surface modifications have significant effect on the compressive strength of the composite foams. For p-CB/PU and o-CB, with the increase of CB contents, the compressive strengths decreased. However, the compressive strength of g-CB/PU foams was obviously higher than those of p-CB/PU and o-CB/PU foams at the same filler content due to the stronger interfacial interactions between g-CB and the PU matrix.

The morphology and distributions of the cell sizes for p-CB/PU foams are shown in Fig. 8, and the average cell

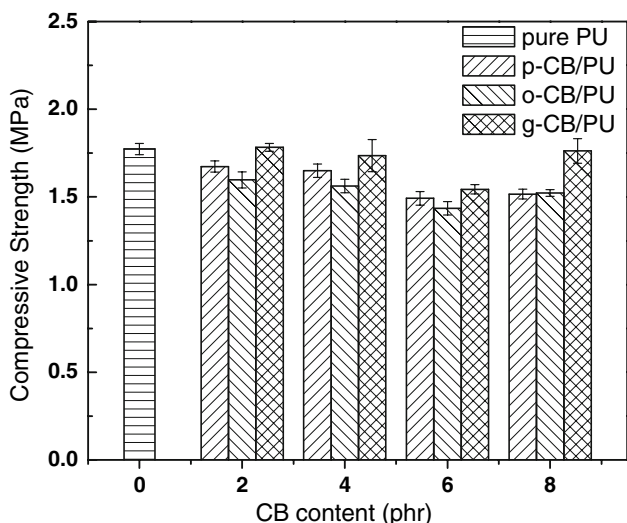


Fig. 7 Compressive strength of p-CB/PU, o-CB/PU, and g-CB/PU foams for different CB contents

sizes are summarized in Table 4. There exist large cells with diameters above 600 μm for pure PU. However, for CB/PU foams, no such large cells are observed in the SEM images (Fig. 9), indicating that CB can prevent the coagulation of small cells during the foaming process. Compared with p-CB/PU foams, the o-CB/PU and g-CB/PU foams have smaller cell sizes, and the size distributions are narrower than those of p-CB/PU. Well-dispersed CB may serve as the nucleation sites during the foaming process to facilitate the bubble nucleation process and produce finer cell structures [36]. o-CB and g-CB have smaller aggregate sizes (Fig. 4) which provide more nucleation sites, leading to a reduction of cell sizes. The g-CB/PU foams have the smallest average cell size and the narrowest size distributions, indicating that surface grafting reaction is more effective for the homogenous dispersion of CB and the reduction of cell sizes than oxidation. Furthermore, it can be concluded from Table 3 that surface modification has a strong effect on the cell sizes, while the variation of CB content seems to have very limited effect on the cell sizes.

Fig. 8 Cell morphology and the distribution of cell sizes of pure PU

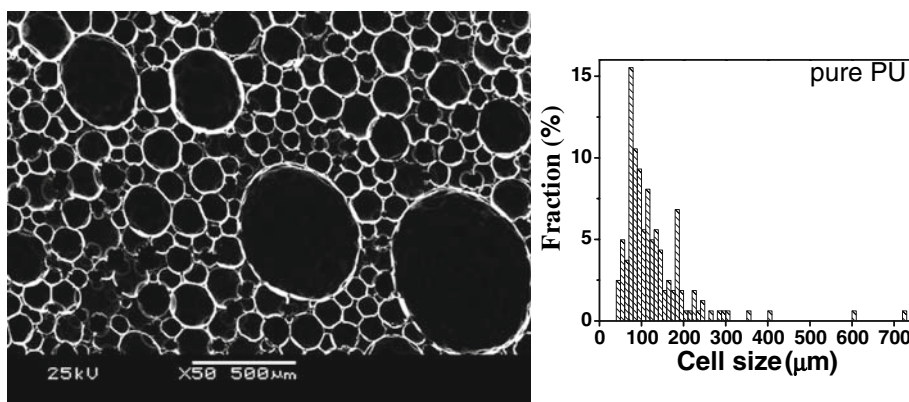


Table 4 Average cell sizes of p-CB/PU, o-CB/PU, and g-CB/PU foams

CB content	Average cell size (μm)		
	p-CB/PU	o-CB/PU	g-CB/PU
0 phr	-	129	-
2 phr	124	108	103
4 phr	115	108	105
6 phr	115	110	104
8 phr	110	105	105

A possible explanation is that the distribution of g-CB in PU is significantly improved, and at filler content as low as 2 phr, the nucleation effect of g-CB is strong enough, so at higher filler contents, the cell size is mainly dominated by other factors such as foaming agent, surfactant, etc. Therefore, with the increase of g-CB concentration, the cell sizes do not exhibit variation.

Conclusions

Surface modifications of CB had significant influences on the structure and properties of CB/PU foams. The dispersion of o-CB and g-CB in polyether polyol and in their CB/PU foams was greatly improved. Owing to the relatively homogenous dispersion, o-CB significantly improved the conductivity of the composite foams. When the content of o-CB was 8 phr, the volume resistivity of o-CB/PU foams was below $10^9 \Omega \text{ m}$. At relatively high filler contents, the resistivity of g-CB/PU foams was lower than that of p-CB/PU foams, but higher than that of o-CB/PU foams, indicating that the grafted polyol on the surface of g-CB reduces the conductivity of the composite foams. The storage moduli of the composite foams were greatly increased, and the glass transition temperatures shifted to higher temperatures for the o-CB/PU and g-CB/PU foams. Owing to the improved dispersion of g-CB particles and the interactions between g-CB particles and the PU matrix,

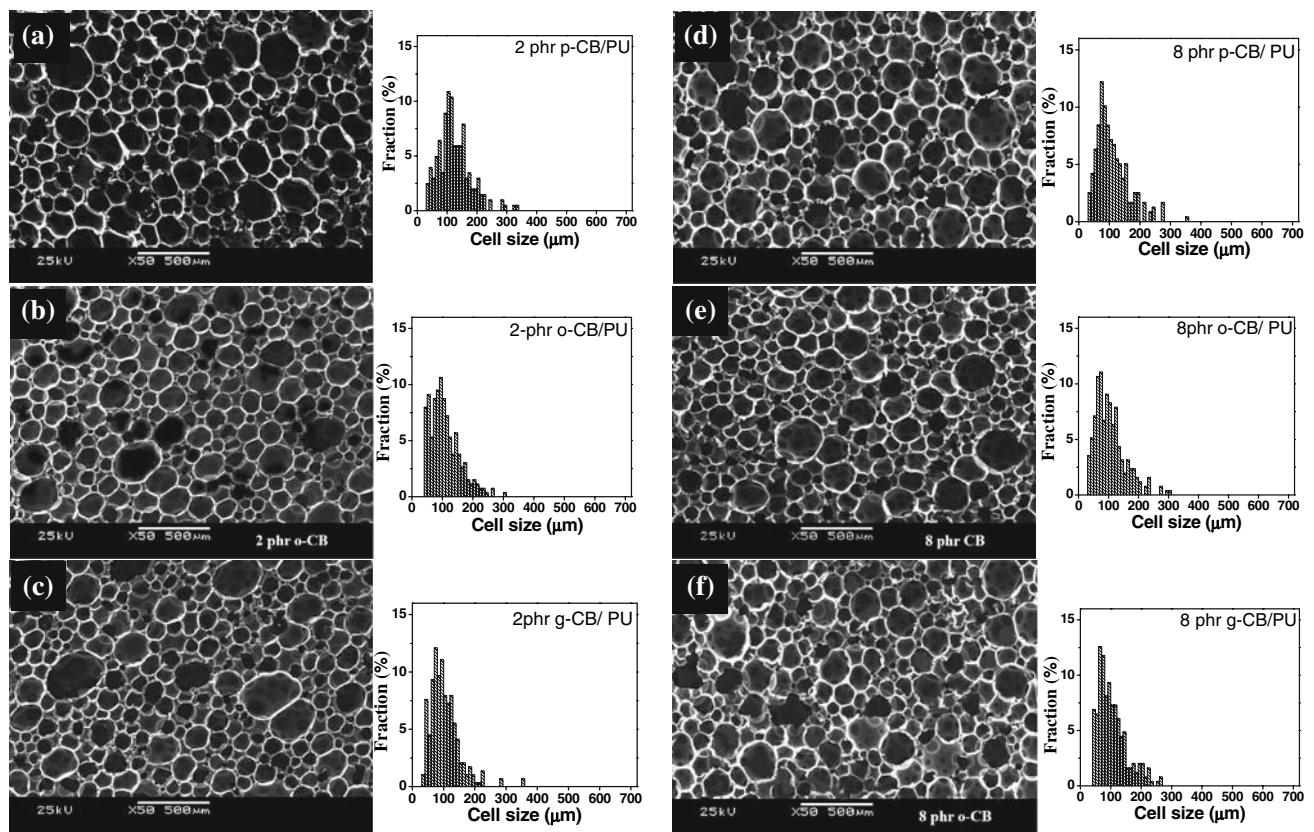


Fig. 9 Cell morphology and the distributions of cell sizes of **a** p-CB/PU, **b** o-CB/PU, and **c** g-CB/PU at a filler content of 2 phr and **d** p-CB/PU, **e** g-CB/PU, and **f** g-CB/PU at a filler content of 8 phr

the g-CB/PU foams showed the best compressive strengths. Furthermore, o-CB/PU and g-CB/PU foams had both smaller cell sizes and narrower size distributions than the p-CB/PU foams, especially for the g-CB/PU foams.

Acknowledgment We appreciate the financial support from National Natural Science Foundation of China (20574060 and 50773066).

References

- Suh KW, Park CP, Maurer MJ et al (2000) *Adv Mater* 12:1779
- Wang Y, Sotzing GA, Weiss RA (2008) *Chem Mater* 20:2574
- Bil M, Ryszkowska J, Kurzydowski KJ (2009) *J Mater Sci* 44:1469. doi:10.1007/s10853-008-3037-8
- Verdejo R, Jell G, Safinia L, Bismarck A, Stevens MM, Shaffer MSP (2009) *J Biomed Mater Res A* 88:65
- Alonso MV, Auad ML, Nutt S (2006) *Compos Part A: Appl Sci Manuf* 37:1952
- Wouterson EM, Boey FYC, Hu X, Wong S (2007) *Polymer* 48:3183
- Yang YL, Gupta MC, Dudley KL, Lawrence RW (2005) *Adv Mater* 17:1999
- Xu XB, Li ZM, Shi L, Bian XC, Xiang ZD (2007) *Small* 3:408
- Cao X, Lee LJ, Widya T, Macosko C (2005) *Polymer* 46:775
- Xu ZB, Tang XL, Gu AJ, Fang ZP (2007) *J Appl Polym Sci* 106:439
- Xu ZB, Tang XL, Gu AJ, Fang ZP, Tong LF (2007) *J Appl Polym Sci* 105:2988
- Song PA, Xu LH, Guo ZH, Zhang Y, Fang ZP (2008) *J Mater Chem* 18:5083
- Cai LF, Huang XB, Rong MZ, Ruan WH, Zhang MQ (2006) *Polymer* 47:7043
- Gelves GA, Lin B, Sundararaj U, Haber JA (2008) *Nanotechnology* 19:215712
- Zhao H, Yuan WZ, Tang L et al (2008) *Macromolecules* 41:8566
- Tian CR, Zhou QM, Wang JH, Zhao XL, Liu J (2003) *China Plast Ind* 31:55
- Kabir ME, Saha MC, Jeelani S (2007) *Mater Sci Eng A* 459:111
- Huang JC (2002) *Adv Polym Technol* 21:299
- Das NC, Maiti S (2008) *J Mater Sci* 43:1920. doi:10.1007/s10853-008-2458-8
- Nigam V, Setua DK, Mathur GN (2001) *J Mater Sci* 36:43. doi:10.1023/A:1004874305070
- Li FK, Qi LY, Yang JP, Xu M, Luo XL et al (2000) *J Appl Polym Sci* 75:68
- Yan B, Deng JR, Wu SQ (2002) *New Chem Mater* 30:26
- Kamegawa K, Nishikubo K, Kodama M, Adachi Y, Yoshida H (2002) *Carbon* 40:1447
- Taniguchi Y, Ogawa M, Gang W et al (2008) *Mater Chem Phys* 108:397
- Boehm HP (1994) *Carbon* 32:759
- Song P, Shen Y, Du B, Peng M, Shen L, Fang Z (2009) *ACS Appl Mater Interfaces* 1:452
- Wang X, Du ZJ, Zhang C, Li CJ, Yang XP, Li HQ (2008) *J Polym Sci. Part A: Polym Chem* 46:4857

28. Han XM, Zeng CC, Lee LJ, Koelling KW, Tomasko DL (2003) *Polym Eng Sci* 43:1261
29. Papirer E, Dentzer J, Li S, Donnet JB (1991) *Carbon* 29:69
30. Beck NV, Meech SE, Norman PR, Pears LA (2002) *Carbon* 40:531
31. Zagar E, Grdadolnik J (2003) *J Mol Struct* 658:143
32. Kamegawa K, Nishikubo K, Yoshida H (1998) *Carbon* 36:433
33. Al-Saleh MH, Sundararaj U (2008) *Compos Part A: Appl Sci Manuf* 39:284
34. Rwei SP, Manas-Zloczower I, Feke DL (1992) *Polym Eng Sci* 32:130
35. Pukanszky B, Moczo J (2004) *Macromol Symp* 214:115
36. Lee LJ, Zeng CC, Cao X, Han XM, Shen J, Xu GJ (2005) *Compos Sci Technol* 65:2344